

Frequency Response-Based Initial Parameter Estimation for SOC of Lithium-Ion Battery

Kohei Natori* Keisuke Mizuno* Toru Namerikawa*
Sabrina Sartori** Frank Eliassen***

* Department of System Design Engineering, Keio University,
Yokohama, 223-8522, Japan (e-mail: namerikawa@sd.keio.ac.jp).

** Department of Technology Systems, University of Oslo, Oslo,
Norway (e-mail: sabrina.sartoei@its.uio.no)

*** Department of Informatics, University of Oslo, Oslo, Norway
(e-mail: frank@ifi.uio.no)

Abstract: In this paper, we propose a novel parameter initial value estimation method of Lithium-ion battery for state of charge (SOC) estimation by using Local Regression Modeling (LRM) and Vector Fitting (VF). To estimate SOC accurately using nonlinear Extended Kalman Filter (EKF), an adequate set of initial parameters of the battery model are required. Therefore, we apply LRM and VF method to derive the initial parameters and the battery model from a constructed database of frequency response data. In addition, we demonstrate the SOC estimation method using EKF by the determined initial value and model. Finally, the effectiveness of the proposed method is shown via several experimental results.

Keywords: battery; SOC; Vector Fitting; Local Regression Modeling; Extended Kalman Filter.

1. INTRODUCTION

In recent years, as interest in energy and environmental problems has increased, massive integration of renewable energy is considered. But renewable energy fluctuates the power generation output due to the weather conditions. Therefore, if large amount of renewable energy is integrated into the power system, the power system will be unstable due to frequency and voltage fluctuations. In order to suppress output fluctuation, introduction of secondary batteries is considered necessary. For this, battery management system (BMS) is necessary for the secure and efficient operation of the secondary battery (Dickson, H. et al. 2019). In this paper, we focus on lithium-ion batteries, a kind of secondary batteries with high energy density and high charge/discharge efficiency, more specifically, we focus on SOC estimation, which is one of the important functions of BMS.

SOC estimation of lithium-ion batteries is executed using the values of measured current, voltage, and temperature. Many researchers have done excellent works related to the SOC estimation method using Kalman filter (Maral, Partovibakhsh. et al. 2015; Htet, Aung. et al. 2015) or H_∞ observer (Cong-zhi, Liu. et al. 2017) and so on. In recent years, a method for simultaneously estimating both SOC and internal impedance of equivalent circuit model was proposed (G, Plett. 2004), which is modeling voltage transients caused by battery open-circuit voltage, current, internal resistance and polarization, and using non-linear Kalman filter such as extended Kalman filter or unscented Kalman filter (G, Plett. 2006). However, when executing estimation using nonlinear Kalman filter, the estimation

accuracy varies greatly depending on the initial value setting. Therefore, some scheme is required for setting the initial value so that the estimation accuracy is improved.

In our previous research (Natori, K. et al. 2015), we dealt with this problem by calculating the initial parameters of the circuit model by using vector fitting (B, Gustavsen. et al. 1999) and applied nonlinear Kalman Filter to the initial parameters. In our previous research, frequency response data is assumed to be obtained in advance just before SOC estimation. However, it takes about 10 minutes to get frequency response data, so it is unrealistic in an experimental environment. In this paper, processing time in a real environment is shortened by obtaining frequency response data under various conditions in advance, constructing the database, and estimating frequency response data at the requested time from database values using local regression modeling proposed in (Shigemori, H. 2010). Estimation of initial parameters is executed to use vector fitting for estimated frequency response data. And SOC estimation is done to apply nonlinear Kalman filter to estimated initial parameters of the equivalent circuit model.

2. PROBLEM FORMULATION

2.1 Battery model

In this paper, we consider the equivalent circuit model of lithium ion battery shown in Fig. 1. R_0 and L is the resistance due to the migration process in the electrolyte and the inductance due to the spiral structure of cylindrical lithium ion, and multiple RC parallel circuits is the resistance due to the charge transfer and diffusion processes. Here, the current direction in which the battery is

charged is positive. At this time, the relational expression derived from the equivalent circuit model is as follows:

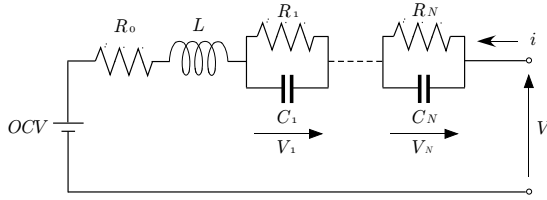


Fig. 1. equivalent circuit model

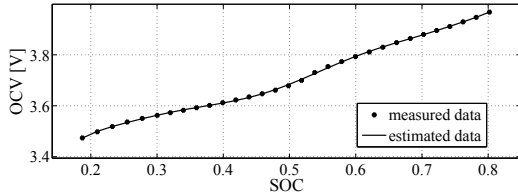


Fig. 2. SOC-OCV characteristic

$$V(t) = OCV(t) + R_0 i(t) + L \frac{di(t)}{dt} + V_1(t) + V_2(t) + \dots + V_N(t) \quad (1)$$

$$\frac{dV_n(t)}{dt}(t) = -\frac{1}{R_n C_n}(t) V_n(t) + \frac{1}{C_n} i(t) \quad (2)$$

($n = 1, 2, \dots, N$)

where OCV is the open-circuit voltage having a relationship with SOC as shown in Fig. 2. This relationship is represented by the approximate function of SOC-OCV characteristics f_{ocv} in (3).

$$OCV(t) = f_{ocv}(SOC(t)) \quad (3)$$

Here $SOC(t)$ is:

$$SOC(t) = SOC(t_0) + \frac{1}{3600 Q_{NC}} \int_{t_0}^t i(\tau) d\tau \quad (4)$$

where t_0 is the estimated start time and Q_{NC} is the rated capacity of the lithium ion battery. The above equations (1)-(4) are discretized by the forward Euler method. The state vector \mathbf{x}_k of the system at time k is defined as follows:

$$\mathbf{x}_k = [SOC_k \ R_{0k} \ L_k \ \mathbf{x}_{1k}^T \ \dots \ \mathbf{x}_{Nk}^T]^T \quad (5)$$

$$\mathbf{x}_{nk} = [V_{nk} \ \frac{1}{R_n C_{nk}} \ \frac{1}{C_{nk}}]^T \quad (6)$$

A discrete-time state equation and observation equation is expressed as follows:

$$\mathbf{x}_{k+1} = \begin{bmatrix} SOC_k + \frac{T_s}{3600 Q_{NC}} i_k \\ R_{0k} \\ L_k \\ \mathbf{X}_{1k} \\ \mathbf{X}_{2k} \\ \vdots \\ \mathbf{X}_{Nk} \end{bmatrix} + \mathbf{w}_k \quad (7)$$

$$\mathbf{x}_{nk} = \begin{bmatrix} \left(1 - T_s \frac{1}{R_n C_{nk}}\right) V_{nk} + T_s \frac{1}{C_{nk}} i_k \\ \frac{1}{R_n C_{nk}} \\ \frac{1}{C_{nk}} \end{bmatrix} \quad (8)$$

$$y_k = f_{ocv}(SOC_k) + R_{0k} i_k + L_k \frac{i_k - i_{k-1}}{T_s} + V_{1k} + V_{2k} + \dots + V_{Nk} + v_k \quad (9)$$

where s is the sampling time[s]. We apply extended Kalman filter for (7)-(9) to estimate SOC. Jacobian $\hat{\mathbf{F}}_k$,

$\hat{\mathbf{H}}_k$ of state equation and observation equation is given as follows.

$$\hat{\mathbf{F}}_k = \begin{bmatrix} 1 & & & & 0 \\ & 1 & & & \\ & & \hat{\mathbf{F}}_{1k} & & \\ & & & \hat{\mathbf{F}}_{2k} & \\ & & & & \ddots \\ 0 & & & & & \hat{\mathbf{F}}_{Nk} \end{bmatrix} \quad (10)$$

$$\hat{\mathbf{F}}_{nk} = \begin{bmatrix} 1 - T_s \cdot \frac{1}{R_n C_{nk}} & -T_s \cdot \frac{1}{C_{nk}} & T_s \cdot i_k \\ 0 & 1 & 0 \\ 0 & 0 & 1 \end{bmatrix}$$

$$\hat{\mathbf{H}}_k = \begin{bmatrix} \frac{df_{ocv}(SOC_k)}{dSOC_k} & i_k & \frac{i_k - i_{k-1}}{T_s} \\ \hat{\mathbf{H}}_{1k} & \hat{\mathbf{H}}_{2k} & \dots & \hat{\mathbf{H}}_{Nk} \end{bmatrix}$$

$$\hat{\mathbf{H}}_{nk} = [1 \ 0 \ 0]$$

The algorithm for the simultaneous estimation method of SOC and parameters applying the extended Kalman filter to the above equation is as follows:

Step 0 : Set the initial value

set initial values of $\hat{\mathbf{x}}_{0|0}$, \mathbf{Q}_0 , R_0 , $\mathbf{P}_{0|0}$

Step 1 : Prediction

$$\hat{\mathbf{x}}_{k+1|k} = \begin{bmatrix} \hat{SOC}_k + \frac{T_s}{3600 Q_{NC}} i_k \\ \hat{R}_{0k} \\ \hat{L}_k \\ \hat{\mathbf{X}}_{1k} \\ \vdots \\ \hat{\mathbf{X}}_{Nk} \end{bmatrix}$$

$$\hat{y}_{k+1} = f_{ocv}(\hat{SOC}_k) + \hat{R}_{0k} i_k + \hat{L}_k \frac{i_k - i_{k-1}}{T_s} + \hat{V}_{1k} + \hat{V}_{2k} + \dots + \hat{V}_{Nk}$$

$$\hat{\mathbf{P}}_{k+1|k} = \hat{\mathbf{F}}_k \mathbf{P}_{k|k} \hat{\mathbf{F}}_k^T + \mathbf{Q}_k$$

Step 2 : Observation

$$\tilde{y}_{k+1|k} = y_k - \hat{y}_{k+1|k}$$

Step 3 : Update

$$\mathbf{K}_{k+1} = \mathbf{P}_{k+1|k} \hat{\mathbf{H}}_k^T [\hat{\mathbf{H}}_k \mathbf{P}_{k+1|k} \hat{\mathbf{H}}_k^T + R_k]^{-1}$$

$$\hat{\mathbf{x}}_{k+1|k+1} = \hat{\mathbf{x}}_{k+1|k} + \mathbf{K}_{k+1} \tilde{y}_{k+1|k}$$

$$\mathbf{P}_{k+1|k+1} = \mathbf{P}_{k+1|k} - \mathbf{K}_{k+1} \hat{\mathbf{H}}_k \mathbf{P}_{k+1|k}$$

where $\mathbf{P}_{k|k}$ is the state error covariance matrix. The accuracy of the simultaneous SOC and parameter estimation method using extended Kalman filter may depend on the initial value of state vector because it is using nonlinear Kalman filter. Therefore, in this paper, we set the main goal as follows to estimate the initial value of the battery's internal impedance of state vector accurately.

Goal

In the simultaneous SOC and parameter estimation method using nonlinear Kalman Filter, the goal is to estimate the initial value of internal impedance close to the true value *without* using frequency response data at the time when SOC estimation is requested. Here, we assume frequency response data acquired in advance under different conditions can be used.

3. INITIAL PARAMETER VALUE ESTIMATION USING THE FREQUENCY RESPONSE DATABASE

In our proposed method, frequency response data under different acquisition conditions are acquired in advance and stored in the database. Frequency response data at the requested time are estimated from data base values by using local regression modeling, and the initial parameter values are estimated using vector fitting for the estimated data.

3.1 Frequency response data estimation using local regression modeling

Local regression modeling (LRM) is a technique to obtain a predicted value by extracting unknown relations between explanatory variables and objective variables from the database, and execute linear approximation to apply multiple regression analysis for the neighborhood of the explanatory variables. We decided to use the local regression model because it can properly linearize the nonlinear relationship between the explanatory variable and the objective variable compared to the global multiple regression model. The frequency response data is known to have strong nonlinearity as shown in Fig. 7.

First, it is known that the frequency response data changes with the charging rate, SOC and temperature, hence the frequency response data are stored in the database when the charging rate SOC and temperature conditions are changing. Next, the acquired conditions are standardized so that the mean is 0 and the variance is 1. Here, the explanatory variable under a certain condition i is set as $\Phi_i = [Z_{SOC\ i} \ Z_T\ i]$, and the real part and imaginal part of frequency response data at K frequency points s_1, \dots, s_K are set as $\mathbf{G}_{R\ i} = [g_{R\ i}(s_1) \ \dots \ g_{R\ i}(s_K)]$, $\mathbf{G}_{I\ i} = [g_{I\ i}(s_1) \ \dots \ g_{I\ i}(s_K)]$. And, database Φ_i , $\mathbf{G}_{R\ i}$, $\mathbf{G}_{I\ i}$ is given as follows, where m is the number of explanatory variable conditions.

$$\phi = [\phi_1^T \ \phi_2^T \ \dots \ \phi_m^T]^T \quad (11)$$

$$\mathbf{G}_R = [\mathbf{G}_{R\ 1}^T \ \mathbf{G}_{R\ 2}^T \ \dots \ \mathbf{G}_{R\ m}^T]^T \quad (12)$$

$$\mathbf{G}_I = [\mathbf{G}_{I\ 1}^T \ \mathbf{G}_{I\ 2}^T \ \dots \ \mathbf{G}_{I\ m}^T]^T \quad (13)$$

From the database ϕ constructed from (11), the neighborhood of the request point for which the initial value is to be predicted is based on the weighted Euclid distance $D(\phi_i, \phi_q) = \sqrt{(\phi_i - \phi_q) W_1 (\phi_i - \phi_q)^T}$, and extract p sets from the ones with small $D(\Theta_i, \Theta_q)$ values. The method of collecting k information vectors in order of distance from the request point is called the k -NN method. Here, the extracted p pairs from the neighborhood are defined as follows:

$$\theta = [\theta_1^T \ \theta_2^T \ \dots \ \theta_p^T]^T \quad (14)$$

$$\mathcal{G}_R = [\mathcal{G}_{R\ 1}^T \ \mathcal{G}_{R\ 2}^T \ \dots \ \mathcal{G}_{R\ p}^T]^T \quad (15)$$

$$\mathcal{G}_I = [\mathcal{G}_{I\ 1}^T \ \mathcal{G}_{I\ 2}^T \ \dots \ \mathcal{G}_{I\ p}^T]^T \quad (16)$$

where $\theta_j = [\mathcal{Z}_{SOC\ j} \ \mathcal{Z}_T\ j]$, and $\mathcal{Z}_{SOC\ j}$ is the standardized value of the database explanatory variable SOC squared, $\mathcal{Z}_T\ j$ is a value standardized by natural logarithm of the explanatory variable T of the database, and $\mathcal{G}_{R\ j}$ and $\mathcal{G}_{I\ j}$ are the real and imaginary parts of the frequency response data corresponding to a certain condition j . For (14) to (16), the weighted multiple regression analysis is used to calculate the real part $\hat{G}_{R\ q}$ and $\hat{G}_{I\ q}$ of the frequency response data at the request point. The weighted multiple regression analysis is expressed as follows:

$$\hat{G}_{R\ q}(s_a) = \theta_q [\Theta^T \Lambda \Theta]^{-1} \Lambda \Theta^T \mathcal{G}_R(s_a) \quad (17)$$

$$\hat{G}_{I\ q}(s_a) = \theta_q [\Theta^T \Lambda \Theta]^{-1} \Lambda \Theta^T \mathcal{G}_I(s_a) \quad (18)$$

$$\Theta = [\mathbf{1} \ \theta] \quad (19)$$

where $\hat{G}_{R\ q}(s_a)$ and $\hat{G}_{I\ q}(s_a)$ are the estimated values of the real and imaginary parts at the frequency point s_a ($a = 1, 2, \dots, K$), and $\mathcal{G}_R(s_a)$ and $\mathcal{G}_I(s_a)$ are the column vector corresponding to the frequency point s_a in \mathcal{G}_R and \mathcal{G}_I . The weight Λ of the weighted multiple regression analysis is as follows:

$$\Lambda = \text{diag}[\Lambda_1 \ \Lambda_2 \ \dots \ \Lambda_p] \quad (20)$$

$$\Lambda_j = \exp(-d(\theta_j, \theta_q)^2) \quad (21)$$

$$D(\theta_j, \theta_q) = \sqrt{(\theta_j - \theta_q) W_2 (\theta_j - \theta_q)^T} \quad (22)$$

By calculating (17) to (19) at all frequency points, the frequency response data at the time when SOC estimation is required can be estimated.

3.2 Parameter initial value estimation using vector fitting

Vector fitting (B, Gustavsen. et al. 1999) is a method for modeling transmission lines inside mobile devices and in-vehicle electronic devices, and approximate frequency characteristics of transmission line with rational function in polar residue form. As a representative method for modeling the inside transmission line, Levenberg-Marquardt method is often used. This method is generally more accurate than vector fitting, but has a high computational cost. In this paper, one of the objectives was to make the processing time in the real environment shorter than the sampling time, so we decided to use vector fitting, which requires a shorter calculation time than the Levenberg-Marquardt method. In vector fitting, consider approximating the frequency response function $F(s)$ with a rational function of order N as follows.

$$F(s) \approx \sum_{n=1}^N \frac{r_n}{s - p_n} + d + s h \quad (23)$$

where, $s = j\omega$, and ω represents the angular frequency. Also, r_n and p_n are real residues and poles, and d and h are real constants terms and proportional terms. Vector fitting is a method of solving by replacing these poles p_n and residues r_n with their respective linear problems. First, the unknown function $\sigma(s)$ is placed as follows, and it is assumed that the product of $\sigma(s)$ and $F(s)$ can be expressed as follows:

$$\sigma(s) = \sum_{n=1}^N \frac{\tilde{r}_n}{s - \tilde{p}_n} + 1 \quad (24)$$

$$\sigma(s)F(s) = \sum_{n=1}^N \frac{r_n}{s - \tilde{p}_n} + d + s h \quad (25)$$

And \tilde{p}_n is the initial pole given as a known value. \tilde{r}_n is an unknown and a residue of $\sigma(s)$. Furthermore, $\sigma(s)$ and $\sigma(s)F(s)$ is assumed to have the same poles. Now, substituting (24) into (25) and rearranging, (26) is obtained.

$$F(s) = \left(\sum_{n=1}^N \frac{r_n}{s - \tilde{p}_n} + d + s h \right) - \left(\sum_{n=1}^N \frac{\tilde{r}_n}{s - \tilde{p}_n} \right) F(s) \quad (26)$$

At this time, since (26) can be regarded as a linear equation with unknown variables r_n, d, h , and \tilde{r}_n , (26) for K measurement points can be expressed as follows:

$$\Psi \mathbf{X} = \mathbf{f} \quad (27)$$

Where Ψ , \mathbf{X} and \mathbf{f} are defined as:

$$\Psi = \begin{bmatrix} \frac{1}{s_1 - \tilde{p}_1} & \cdots & \frac{1}{s_1 - \tilde{p}_N} & 1 & s_1 & -\frac{F(s_1)}{s_1 - \tilde{p}_1} & \cdots & -\frac{F(s_1)}{s_1 - \tilde{p}_N} \\ \vdots & & \vdots & \vdots & \vdots & \vdots & & \vdots \\ \frac{1}{s_K - \tilde{p}_1} & \cdots & \frac{1}{s_K - \tilde{p}_N} & 1 & s_K & -\frac{F(s_K)}{s_K - \tilde{p}_1} & \cdots & -\frac{F(s_K)}{s_K - \tilde{p}_N} \end{bmatrix}$$

$$\mathbf{X} = [r_1 \cdots r_N \ d \ h \ \tilde{r}_1 \cdots \tilde{r}_N]^T$$

$$\mathbf{f} = [F(s_1) \cdots F(s_K)]^T$$

Here, Ψ is a K -by- $2N + 2$ matrix, and if there are enough measurement points, the matrix is an over-determined system. Hence the residue r_n can be obtained by singular value decomposition. Next, if we put $q(s) = \sigma(s)F(s)$, $q(s)$ and $\sigma(s)$ can be expressed as follows:

$$q(s) = h \frac{\prod_{n=1}^{N+1} (s - z_n)}{\prod_{n=1}^N (s - \tilde{p}_n)} \quad (28)$$

$$\sigma(s) = \frac{\prod_{n=1}^N (s - \tilde{z}_n)}{\prod_{n=1}^N (s - \tilde{p}_n)} \quad (29)$$

where z_n and \tilde{z}_n are the zero points of $q(s)$ and $\sigma(s)$, respectively. Both are unknown. From (26) and (27), $F(s)$ is transformed into:

$$F(s) = \frac{q(s)}{\sigma(s)} = h \frac{\prod_{n=1}^N (s - z_n)}{\prod_{n=1}^N (s - \tilde{z}_n)} \quad (30)$$

Here, comparing (23) and (30), it is clear that the pole p_n of $F(s)$ is equal to the zero point \tilde{z}_n of $\sigma(s)$, and if the zero point \tilde{z}_n of $\sigma(s)$ can be calculated, the pole p_n of $F(s)$ can also be calculated. Therefore, we obtain the pole p_n of $F(s)$ by calculating the zero point \tilde{z}_n of $\sigma(s)$. As a method of calculating the zero point \tilde{z}_n of $\sigma(s)$, we use the fact that the eigenvalues of the following matrix correspond to the zero point \tilde{z}_n of $\sigma(s)$. In short, the pole p_n (zero point \tilde{z}_n) of $F(s)$ can be obtained by finding the eigenvalue of (31).

$$\mathbf{Q} = \hat{\mathbf{A}} - \hat{\mathbf{b}} \cdot \hat{\mathbf{c}}^T \quad (31)$$

where $\hat{\mathbf{A}}$ is a diagonal matrix with the initial pole \tilde{p}_n as a diagonal element, $\hat{\mathbf{b}}$ is a column vector with all elements 1 and $\hat{\mathbf{c}}^T$ is a row vector with elements as a residue \tilde{r}_n of $\sigma(s)$ obtained by solving (27). The pole p_n obtained above is not an exact solution because it uses \tilde{p}_n given as the initial pole. Therefore, the obtained eigenvalue (pole p_n) is replaced with the initial pole and (27) is solved again, and the eigenvalue of (31) is calculated using the new \tilde{p}_n obtained by solving (27). By repeating this procedure, the pole approaches the true value. In summary, the vector fitting algorithm is as follows.

Step 0 : Set the initial pole

give the initial pole \tilde{p}_n ($n = 1, 2, \dots, N$)

Step 1 : Calculate residue r_n and d, h

Calculate the residue r_n , constant term d , and proportional term h by singular value decomposition of the least squares solution

Step 2 : Calculate pole p_n

Calculate pole p_n by finding eigenvalue of (31)

The frequency response approximation function $F(s)$ can be obtained by repeating Step 1 and 2 above.

Consider the correspondence relationship between the frequency response approximation function $F(s)$ calculated by vector fitting and the equivalent circuit model in Fig. 5. To apply Laplace transform for each of the

passive elements of resistor R , inductor L , and parallel circuit $R_p C_p$ as shown in Fig. 5, we can obtain relational expression as (32)-(34).

$$V(s) = R I(s) \quad (32)$$

$$V(s) = sL I(s) \quad (33)$$

$$V(s) = \frac{R_p}{sR_p C_p + 1} I(s) = \frac{\frac{1}{C_p}}{s + \frac{1}{R_p C_p}} I(s) \quad (34)$$

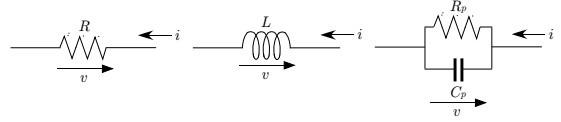


Fig. 3. Passive circuits

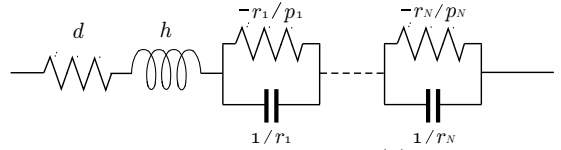


Fig. 4. Equivalent circuit model of $F(s)$

Here, comparing (23) with (32) to (34), we can find that the constant term d corresponds to the resistor, the proportional term h corresponds to the inductor, and the fractional expression $\frac{r_n}{s - p_n}$ corresponds to the multiple RC parallel circuits. Therefore, if the frequency response function $F(s)$ can be derived, the entire internal impedance part of Fig. 1 can be expressed as shown in Fig. 6. In this paper, the initial value of the internal impedance can be estimated from the frequency response data by using vector fitting with the frequency response data estimate obtained in the previous section $\hat{\mathbf{G}}_q = \hat{\mathbf{G}}_{Rq} + i \hat{\mathbf{G}}_{Iq}$ as $F(s)$.

4. VERIFICATION BASED ON EXPERIMENTAL DATABASE

4.1 Experimental conditions

We explain about the flow of data collection experiments. First, the sample battery is charged by constant current of 1[A] until the voltage value is set to $V = 4.2V$. After that, the battery is charged for 3 hours with constant voltage of 4.2[V]. In this paper, this charging state is called fully charge state, that is, $SOC = 1.0$, and the value of SOC in the subsequent experiments is calculated by current integration method. After the fully charged state is reached, constant current discharge is executed from the fully charged state, we collected frequency response data for database used for local regression modeling under each condition, that SOC is in the range 0.3 to 0.8 in increments of 0.02(26 data), and temperature is in the range 15 to 30[°C] in increments of 5[°C](4 data). That is, the condition number of the explanatory variables is $26 \times 4 = 104$. Along with the above frequency response data acquisition experiment, the open-circuit voltage was obtained when the SOC was varied in the range of 0.8 to 0.3 in a constant temperature bath at a constant temperature of 25 degrees, and the SOC-OCV characteristics graph was obtained (see Fig. 2). The graph of SOC-OCV characteristics approximate function $f_{ocv}(SOC)$ is obtained using multiple regression analysis. The average error rate of approximate function in (35) is 2.83×10^{-5} and accurate approximation is achieved.

$$\begin{aligned}
 f_{ocv}(SOC) = & 2.96 \times 10^4 SOC^{10} - 1.35 \times 10^5 SOC^9 \\
 & + 2.66 \times 10^5 SOC^8 - 2.94 \times 10^5 SOC^7 \\
 & + 1.99 \times 10^5 SOC^6 - 8.52 \times 10^4 SOC^5 \\
 & + 2.24 \times 10^4 SOC^4 - 3.26 \times 10^3 SOC^3 \\
 & + 1.56 \times 10^2 SOC^2 + 1.90 \times 10^1 SOC + 1.32 \quad (35)
 \end{aligned}$$

Furthermore, in order to verify the effectiveness of the proposed method, a discharge experiment was performed in which 1[A] constant current discharge was repeatedly performed every 180[s] from the initial conditions determined randomly as shown in Table 1. In addition, frequency response data under each condition was acquired just before the discharge experiment. Fig. 5 shows the current obtained in the discharge experiment, Fig. 6 shows the voltage, Fig. 7 shows the frequency response data. And the order of the RC parallel circuit is set $N = 5$.

Table 1. Conditions of experimental data

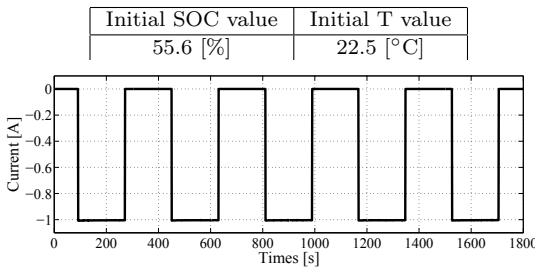


Fig. 5. Current time response of discharge

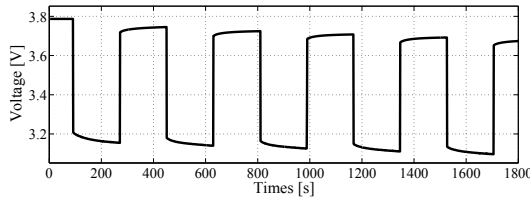


Fig. 6. Voltage time response of discharge

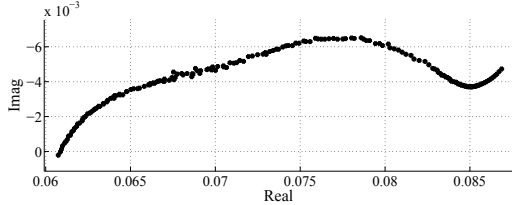


Fig. 7. Frequency response

4.2 Internal impedance initial value estimation result

The results of estimating the frequency response data using the proposed method are shown below. Also the design parameters used in the proposed method in this paper are shown in the following. The k -division cross-validation method was adopted for all the frequency response data for the database acquired in the previous section, and it was determined as follows by trial and error.

$$q = 16 \quad (36)$$

$$W_1 = \begin{bmatrix} 1 & 0 \\ 0 & 0.08 \end{bmatrix}, W_2 = \begin{bmatrix} 1 & 0 \\ 0 & 1.2 \end{bmatrix} \quad (37)$$

$$\tilde{p}_1 = -0.1, \tilde{p}_2 = -1, \tilde{p}_3 = -10, \tilde{p}_4 = -50, \tilde{p}_5 = -1000 \quad (38)$$

Fig. 9 shows the results of estimation by the proposed method using the above design parameters. As can be seen from this figure, it is confirmed that the shape of the frequency response data can be imitated. In addition,

the estimation time of the frequency response data in this paper (calculation time by the proposed method) is about 0.02 [s], which is shorter than the sampling time 1 [s] of the current and voltage values. Hence it can be said to be realistic. The estimated internal impedance obtained by the proposed method is effective.

4.3 SOC estimation result

The results of SOC estimation using the initial value of the internal impedance estimated in the previous section are shown below. The design parameters used for the extended Kalman Filter in this paper are also shown in the following. The value of $Q_0, R_0, P_{0|0}$ under each condition was determined by trial and error as follows.

$$\begin{aligned}
 Q_0 = & \text{diag}[10^{-3} \ 10^{-3} \ 10^{-8} \ 10^{-4} \ 10^2 \ 10^0 \\
 & 10^{-4} \ 10^2 \ 10^{-2} \ 10^{-4} \ 10^2 \ 10^{-2} \\
 & 10^{-3} \ 10^0 \ 10^{-4} \ 10^{-3} \ 10^{-2} \ 10^{-5}]^T
 \end{aligned}$$

$$R_0 = 1.0 \times 10^{-4}$$

$$\begin{aligned}
 P_{0|0} = & \text{diag}[10^{-2} \ 10^{-3} \ 10^{-6} \ 10^6 \ 10^3 \ 10^0 \\
 & 10^6 \ 10^3 \ 10^{-1} \ 10^6 \ 10^0 \ 10^{-3} \\
 & 10^6 \ 10^{-1} \ 10^{-4} \ 10^6 \ 10^{-2} \ 10^{-6}]^T
 \end{aligned}$$

Using the above design parameters, the SOC estimation results under each condition are shown in Fig. 10, and the error from the true value is shown in Fig. 11, and Fig. 12 shows the estimation errors of the comparison target and the proposed method. In addition, using unsuitable design parameters ($5Q_0, 5R_0, 5P_{0|0}$), the estimation results of SOC under each condition are shown in Fig. 13, and the error from the true value is shown in Fig. 14, respectively, and the estimation error of the comparison target and the proposed method are shown in Fig. 15, respectively.

However, as a comparison target for SOC estimation, we used the estimation results using the initial values estimated by applying vector fitting to the frequency response data (Figs. 9 and 12) acquired immediately before the discharge, and the estimated SOC obtained by the current integration method was adopted (S, Piller. et al. 2010). Looking at Fig. 11, it can be seen that there is a SOC shift due to a shift in the initial value near the

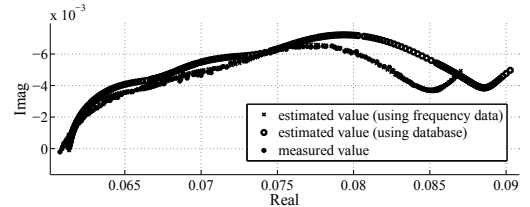


Fig. 8. Frequency response estimation result

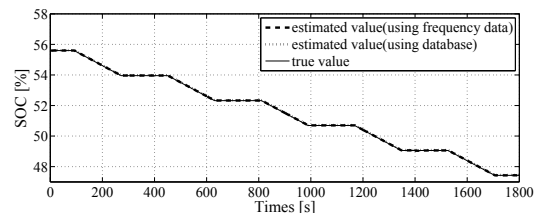


Fig. 9. SOC estimation result

estimated start time. From Fig. 12, when the end time approaches, it can be seen that the estimated value using the proposed method is close to the comparison target. In fact, looking at the result Fig. 14, it can be confirmed that there is an error in the estimated value as the end time is approached for the design parameters that are not appropriate. From this, it was confirmed that the error of the initial value of internal impedance can be reduced by giving appropriate design parameters Q_0 , R_0 , and $P_{0|0}$. From the above, it can be concluded that the internal impedance initial value estimated by the proposed method can be used for the SOC and parameter simultaneous estimation method by nonlinear Kalman Filter.

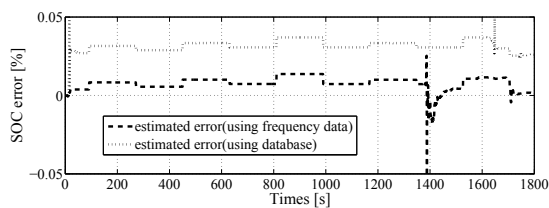


Fig. 10. SOC estimation error

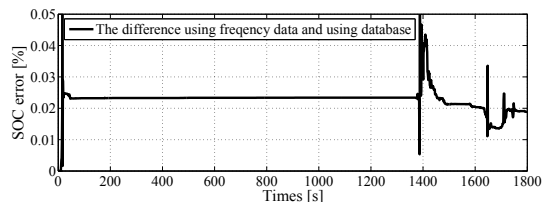


Fig. 11 The difference frequency data and database

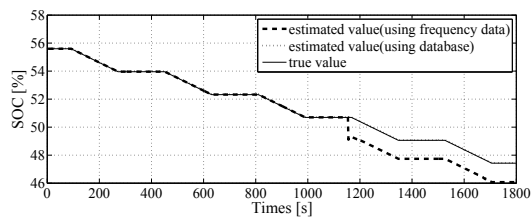


Fig. 12. SOC estimation result

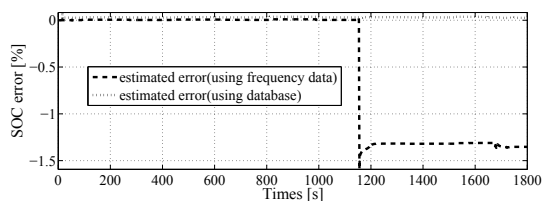


Fig. 13. SOC estimation error

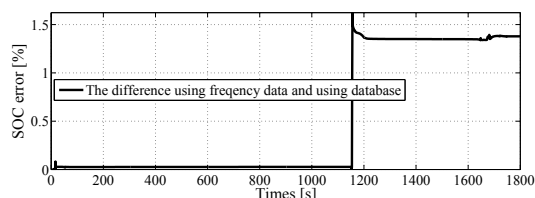


Fig. 14. The difference frequency data and database

5. CONCLUSION

In this paper, we focused on the the estimation of SOC of lithium-ion batteries, and proposed the method for estimating the initial value of internal impedance using high-order equivalent circuit model. In the proposed method, we

collected the frequency response data when the SOC and temperature conditions are changing and constructed the database. Next, we estimate the initial value of the internal impedance by estimating the frequency response data at the time using the database and local regression modeling at the time when the SOC estimation request was made, and applying vector fitting to the estimated value. In the verification of the effectiveness using experimental data, the internal impedance initial value and the SOC were estimated using the discharge experimental data under two randomly determined conditions. The internal impedance initial value estimation results suggest that the proposed method is effective for initial value estimation, and we find that the internal impedance initial values estimated by the proposed method from the SOC estimation results can be applied to the SOC and parameter simultaneous estimation method using a nonlinear Kalman filter.

REFERENCES

- Dickson, H., & M, Hannan., & M, Lipu., & Pin, Ker. (2019). State of Charge Estimation for Lithium-Ion Batteries Using Model-Based and Data-Driven Methods: A Review , *IEEE Trans. on Access*, 7(1), 136116–136136.
- Maral, Partovibakhsh., & Guangjun, Liu. (2015). An Adaptive Unscented Kalman Filtering Approach for Online Estimation of Model Parameters and State-of-Charge of Lithium-Ion Batteries for Autonomous Mobile Robots , *IEEE Trans. on Control Systems Technology*, 23(1), 357–363.
- Htet, Aung., & Kay, Soon, Low., & Shu, Ting, Goh., (2015). State-of-Charge Estimation of Lithium-Ion Battery Using Square Root Spherical Unscented Kalman Filter (Sqrt-UKFST) in Nanosatellite , *IEEE Trans. on Power Electronics*, 30(9), 4774–4783.
- Cong-zhi, Liu., & Qiao, Zhu., & Wei-qun, Liu., & Ling-Yan, Wang., & Neng, Xiong., & Xiang-yu, Wang., (2017). A State of Charge Estimation Method Based on H_∞ Observer for Switched Systems of Lithium-Ion Nickel–Manganese–Cobalt Batteries , *IEEE Trans. on Industrial Electronics*, 64(10), 8128–8137.
- G, Plett. (2004). Extended Kalman filtering for battery management systems of LiPB-based HEV battery packs: Part 3. State and parameter estimation , *Journal of Power Sources*, 134(2), 277–292.
- G, Plett. (2004). Sigma-point Kalman filtering for battery management systems of LiPB-based HEV battery packs: Part 2: Simultaneous state and parameter estimation , *Journal of Power Sources*, 161(2), 1369–1384.
- Natori, K., & Namerikawa, T. (2015). Estimation of State of Charge for Lithium-Ion Battery using Vector Fitting and Kalman Filter , *Automatic Control Federation Lecture*, 1C2(2).
- B, Gustavsen., & A, Semlyen. (1999). Rational approximation of frequency domain responses by vector fitting, *IEEE Transactions on Power Delivery*, 14(3), 1052–1061.
- Shigemori, H. (2010). Practical application of steel quality control by local regression model , *Journal of measurement and control*, 49(7), 439–443.
- S, Piller., & M, Perrin., & A, Jossen., (2001). Methods for state-of-charge determination and their applications, *Journal of power sources*, 96(1), 113–120.